



# A TGA–DSC-based study on macroscopic behaviors of coal–oxygen reactions in context of underground coal fires

Jun Li<sup>1,2</sup> · Yinan Yang<sup>1,2</sup> · Jinsong Li<sup>1,2</sup> · Yandong Mao<sup>3</sup> · Varinder Saini<sup>4</sup> · Svetlana Kokh<sup>5</sup>

Received: 18 October 2020 / Accepted: 9 February 2021 / Published online: 13 March 2021  
© Akadémiai Kiadó, Budapest, Hungary 2021

## Abstract

Underground coal fires (UCFs) cause remarkable loss of energy resources and significant environmental pollution. Due to the limited capacity of oxygen transport, the inception and development of UCFs represent a very unique mode of coal–oxygen reactions. Therefore, a high-volatile flammable coal sample is thermally analyzed with the combined TGA–DSC approach under four oxygen concentrations (21%, 15%, 9% and 3%) and three heating rates (1 °C min<sup>-1</sup>, 2 °C min<sup>-1</sup> and 5 °C min<sup>-1</sup>). It is found that the oxygen concentration does not significantly influence the early (low-temperature) stage of coal–oxygen reactions. With the decrease in oxygen concentration, the intensity of the exothermic reactions is reduced and the duration of reactions is extended. Based on the experimental results, the apparent activation energy is calculated. The variation of the apparent activation energy reflects the different reaction stages: volatiles burning and char oxidation, which is verified by the TGA–DSC results. Under the extreme condition of 3% oxygen concentration, a very distinct macroscopic thermochemical behavior is observed, and the limited oxygen supply controls the reaction rate throughout the entire process, which qualitatively explains the persistency of the burning phenomena in most UCFs.

**Keywords** Underground coal fires · Coal–oxygen reactions · Oxygen concentration · Heating rate · TGA–DSC · Apparent activation energy

## Introduction

Underground coal fires (UCFs) cause serious harms to natural coal resources, environment, human health and mining safety [1, 2]. UCFs have been continuously burning in most

coal-producing countries such as China, the USA, Australia, India and many others [3]. At the early stage of UCFs, they are usually very difficult to be detected; once found, they are extremely difficult to be completely extinguished. The ignition and burning processes in UCFs represent a very unique combustion mode different from other commonly encountered scenarios such as pulverized particles or fluidized bed. The understanding of the inception and development is important to the effective prevention and control of UCFs [4, 5].

UCFs are a very persistent burning phenomenon and involve many physical and chemical processes. It is generally agreed that their inception is attributed to heat accumulation from the low-temperature oxidation of coal, which has been extensively discussed in previous studies [6–9]. Basically, the understanding of low-temperature reactions aims to help the prevention of UCFs at their early stage. In those studies, the products from coal–oxygen reactions [10, 11] and some parameters such as the heat release [12], the particle size [13, 14] and chemical kinetics [15, 16] have been investigated. Heat accumulation over time leads to the temperature rise and ultimately gives rise to spontaneous

✉ Jun Li  
lijun79@tju.edu.cn

<sup>1</sup> Key Laboratory of Efficient Utilization of Low and Medium Grade Energy, Ministry of Education, Tianjin University, Tianjin 300350, China

<sup>2</sup> Department of Energy and Power Engineering, School of Mechanical Engineering, Tianjin University, Tianjin 300350, China

<sup>3</sup> State Key Laboratory of Coal-Based Low Carbon Energy, Enn Technology and Development Co. Ltd., Langfang Hebei Province 065001, China

<sup>4</sup> Department of Civil Engineering, Indian Institute of Technology Ropar, Rupnagar, Punjab 140001, India

<sup>5</sup> Institute of Mineralogy and Petrography, Geophysics and Mineralogy, United Institute of Geology, Siberian Branch of the Russian Academy of Sciences, Novosibirsk 630090, Russia

combustion, also known as ‘self-ignition’ [17, 18]. The self-heating stage could usually last a very long time. Typically, air supply to the burning zone in the coal seam is in the form of seepage flows through porous media such as soil, sand, rock and other types of geological formations. Natural convection is the dominant driving force enabling seepage flows in UCFs [19, 20]. Once the coal–oxygen reactions enter the high-temperature regime, compared to the low-temperature oxidation, oxygen transport becomes a major limiting factor that controls the reaction rate, and as a result smoldering combustion is the typical burning mode in most UCFs [21, 22]. Flaming combustion could also occur in some cases if sufficient air supply is feasible, for example, shallowly buried coal seams with open holes or through fractures/fissures in the overburden allowing direct contact to the atmosphere [23]. Due to the temporal and spatial variation of air flow conditions, coal–oxygen reactions proceed with variant oxygen concentrations, leading to some unique macroscopic behaviors which we have insufficiently understood so far. Established knowledge of coal burning in other energy and chemical industries could not be directly applied in the context of UCFs in view of their significant difference in terms of oxygen transport.

To quantitatively characterize the chemical kinetics and thermal behaviors of coal–oxygen reactions under different conditions, the thermogravimetric analysis (TGA) and

differential scanning calorimetry (DSC) have been widely applied [24, 25]. As mentioned above, in the context of UCFs the oxygen concentration is a major variable influencing the intensity of coal–oxygen reactions [21]. Also, at different stages, the rate of temperature rise also varies in magnitude. For example, the temperature rise is very slow ( $<< 1\text{ }^{\circ}\text{C min}^{-1}$ ) during the low-temperature oxidation of coal, while at the high-temperature stage, it could reach several degrees per minute. Over such a wide span, it is almost impossible to obtain detailed reaction pathways (elementary reactions). Thus, it is more practical and feasible to focus on the macroscopic behaviors of coal–oxygen reactions. Table 1 summarizes some relevant studies found in the open literature dealing with the two factors mentioned above: the oxygen concentration and the heating rate. However, less considerations were given in these studies in view of the actual reaction conditions of UCFs. Li et al. [26] designed a laboratory-scale experimental setup to simulate actual UCFs driven by natural convection, and their measurement results indicate that at the early stage of coal–oxygen reactions, the temperature changing rate is very low ( $\sim 1\text{ }^{\circ}\text{C min}^{-1}$ ). Figure 1 shows the temporal evolution of coal temperature and its changing rate. Throughout the process, the maximum temperature changing rate is no higher than  $3\text{ }^{\circ}\text{C min}^{-1}$ . Therefore, the present study employs more reasonable heating rates in the thermal analysis. As to the other factor, that

**Table 1** Summary of previous studies and the present study

References	Coal rank (volatile)	Heating rate	Oxygen concentration	Temperature	Diameter	Mass	Testing method
[28]	Jet coal (30.01%) Gas coal (34.82%) Fat coal (26.71%)	$5\text{ }^{\circ}\text{C min}^{-1}$	21%, 19%, 16%, 13%, 10%, 7%, 5%	RT–1000 $^{\circ}\text{C}$	0.18–0.38 mm	8 mg	TGA
[29]	Brown coal (47.45%)	$0.5\text{ }^{\circ}\text{C min}^{-1}$ $1\text{ }^{\circ}\text{C min}^{-1}$ $2.5\text{ }^{\circ}\text{C min}^{-1}$ $5\text{ }^{\circ}\text{C min}^{-1}$	Nitrogen condition Air condition	30–230 $^{\circ}\text{C}$	0.125–0.25 mm	3–20 mg	DSC
[30]	Lean coal (15.63%) Jet coal (28.61%) Gas coal (30.61%)	$5\text{ }^{\circ}\text{C min}^{-1}$ $10\text{ }^{\circ}\text{C min}^{-1}$ $15\text{ }^{\circ}\text{C min}^{-1}$	21%, 17%, 13%, 9%, 5%	30–950 $^{\circ}\text{C}$	0.08–0.096 mm	10 mg	TGA
[27]	Jet coal (29.42%) Meager coal (11.33%)	$0.1\text{ }^{\circ}\text{C min}^{-1}$	21%, 15%, 10%, 5%, 3% Nitrogen condition	RT–200 $^{\circ}\text{C}$	0.075–0.15 mm	1000 mg	DSC
[31]	Lean coal (15.63%) Coking coal (13.59%) Jet coal (45.26%)	$5\text{ }^{\circ}\text{C min}^{-1}$ $10\text{ }^{\circ}\text{C min}^{-1}$ $15\text{ }^{\circ}\text{C min}^{-1}$	Air condition	30–950 $^{\circ}\text{C}$	0.08–0.096 mm	10 mg	TGA
[32]	Gas coal (34.44%)	$1\text{ }^{\circ}\text{C min}^{-1}$ $2.5\text{ }^{\circ}\text{C min}^{-1}$ $5\text{ }^{\circ}\text{C min}^{-1}$ $10\text{ }^{\circ}\text{C min}^{-1}$	Air condition	RT–800 $^{\circ}\text{C}$	0.125–0.25 mm 0.25–0.5 mm 0.5–0.71 mm	20 mg	TGA–DSC
Present study	Brown coal (43.27%)	$1\text{ }^{\circ}\text{C min}^{-1}$ $2\text{ }^{\circ}\text{C min}^{-1}$ $5\text{ }^{\circ}\text{C min}^{-1}$	21%, 15%, 9%, 3%	30–600 $^{\circ}\text{C}$ 30–960 $^{\circ}\text{C}$ 30–1200 $^{\circ}\text{C}$	< 1 mm	30 mg	TGA–DSC

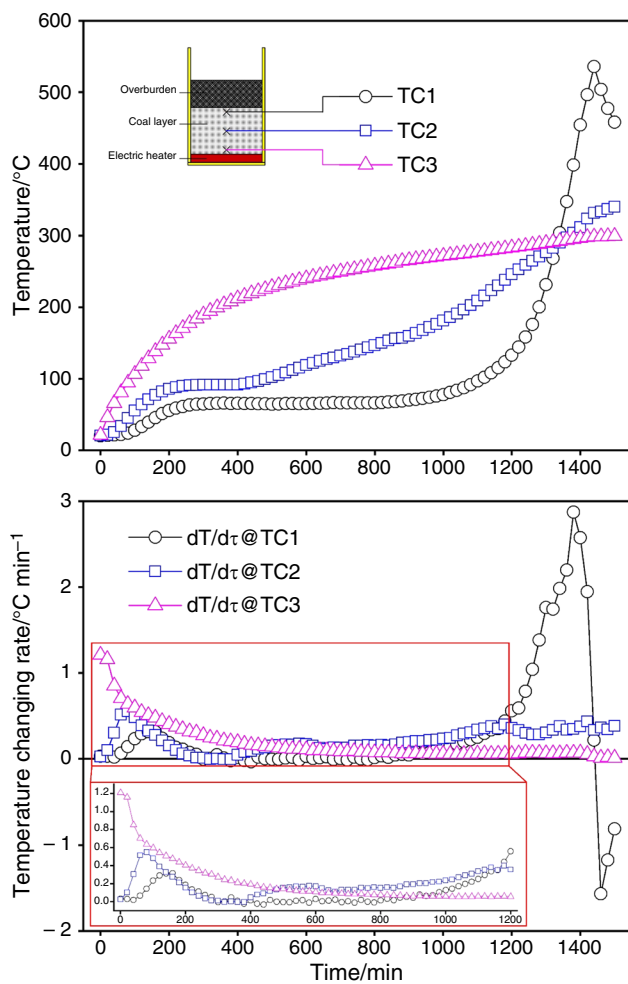


**Fig. 1** Temporal evolution of coal temperature and its changing rate (adapted from Ref. [26] with TC denoting thermocouple)

is, the oxygen concentration, coal fires usually occur in the longwall gob areas where the oxygen concentration is lower than 21% [27]. During the process of prevention and control UCFs, nitrogen injection into the fire zone is a conventional measure adopted by most coal mines. According to the latest amended ‘Coal Mine Safety Regulation (2016) of China’, when nitrogen is used to extinguish UCFs, the nitrogen concentration should not be lower than 97%, meaning that the coal could still be exposed to an oxygen concentration of ~3%. Based on that information, the lowest oxygen concentration is determined to be 3% in such testing cases. It is believed that the present study is more applicable to the conditions of actual UCFs.

In summary, the present study will employ the combined TGA–DSC approach to systematically investigate the reaction rates and thermal behaviors of a given coal sample. The results will be analyzed with the target to quantify the apparent activation energy at different stages of coal–oxygen reactions. It should be stressed that the primary objective of

the present study is to understand the macroscopic behaviors of coal–oxygen reactions under the conditions derived from actual UCFs. Discussions on the effect of the oxygen concentration will also be carried out.

## Experimental

### Coal sample

It is estimated that in China, brown coal (only reserves) accounts for ~13% of the country’s total, but the danger of that coal to self-ignition is prominent [33]. Therefore, a high-volatile flammable brown coal which is obtained from Hami of Xinjiang Uyghur Autonomous Region, China, is used in the present study. Its proximate and ultimate analyses are given in Tables 2 and 3, respectively. Prior to the tests, the raw coal was crushed into particles of <1 mm in diameter and stored in a sealed container to prevent the contact with air. The present study considers the influence of water in the coal sample, and therefore drying is not applied before the tests.

### Testing system and procedure

The TGA–DSC tests are carried out on the METTLER TOLEDO® TGA/DSC 1/1600 Analyzer whose measurement accuracy of mass and temperature are 0.0001 mg and ±0.5 °C, respectively. About 30 mg of coal sample is placed in a crucible. Three heating rates (1, 2 and 5 °C min<sup>-1</sup>) are used. As can be seen in Fig. 1, the higher rate of temperature rise only occurs at sufficiently high temperature. Hence, the ending temperatures for the testing cases are determined in a more reasonable way, as shown in Table 4, with 1200 °C, 960 °C and 600 °C for 5 °C min<sup>-1</sup>, 2 °C min<sup>-1</sup> and 1 °C min<sup>-1</sup>, respectively. Two cylinders (nitrogen and oxygen) are used as the source, and two mass

**Table 2** Proximate analysis of coal sample

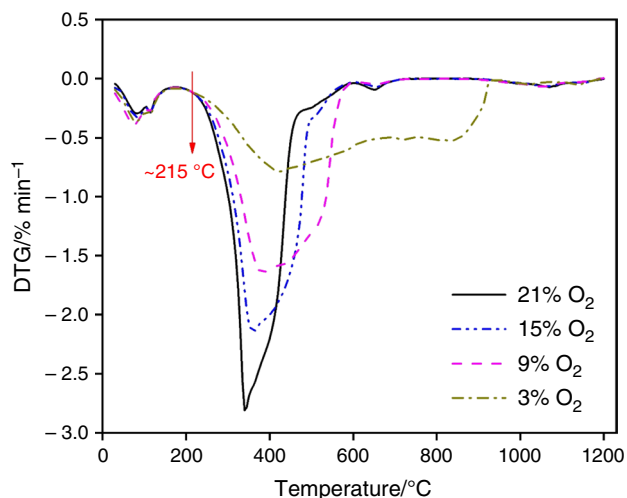
Moisture $M_{ar}/\%$	Moisture $M_{ad}/\%$	Ash $A_d/\%$	Volatile matter $V_d/\%$	Heat content (dry fuel)/MJ kg <sup>-1</sup>	
				Gross calorific value	Net calorific value
23.82	12.71	11.57	43.27	26.084	25.067

**Table 3** Ultimate analysis of coal sample

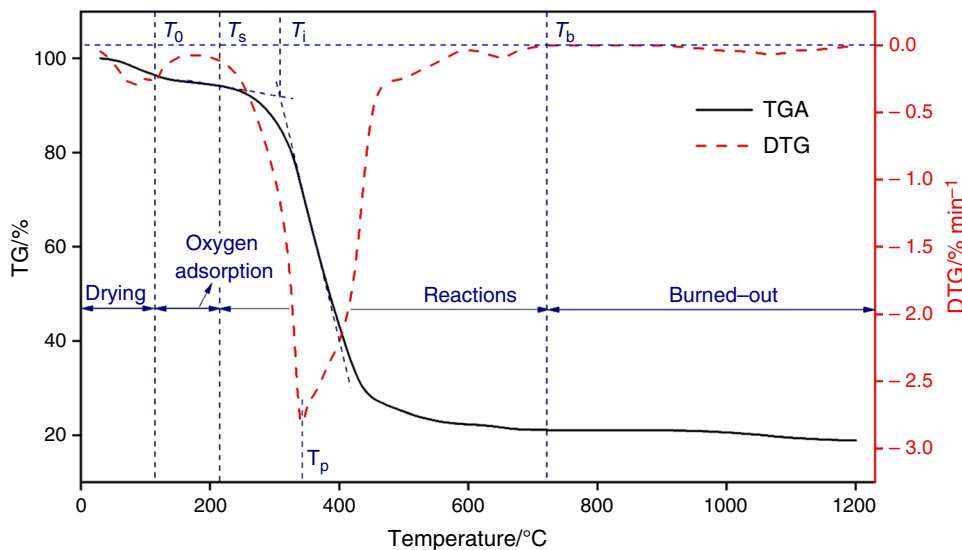
Carbon $C_d/\%$	Hydrogen $H_d/\%$	Nitrogen $N_d/\%$	Sulfur $S_d/\%$
65.39	4.94	0.82	1.18

**Table 4** Testing conditions

Oxygen concentration/%	Temperature range		
	1 °C min <sup>-1</sup>	2 °C min <sup>-1</sup>	5 °C min <sup>-1</sup>
21	30–600 °C	30–960 °C	30–1200 °C
15	30–600 °C	30–960 °C	30–1200 °C
9	30–600 °C	30–960 °C	30–1200 °C
3	30–600 °C	30–960 °C	30–1200 °C

**Fig. 2** DTG results under different oxygen concentrations at 5 °C min<sup>-1</sup> heating rate

flow controllers are applied to achieve the required oxygen concentration. Nitrogen and oxygen are fully mixed before entering the reactor, and a constant flow rate of 50 mL min<sup>-1</sup> is applied throughout all testing cases.

**Fig. 3** TGA–DTG result at 5 °C min<sup>-1</sup> heating rate under 21% oxygen concentration

## Results and discussion

### Thermogravimetric characteristics

The TGA result indicates mass changes over the heating period, while its derivative DTG reflects the changing rate. Figure 2 shows the DTG results for the cases under different oxygen concentrations at the heating rate of 5 °C min<sup>-1</sup>. It can be seen that the four cases start to diverge only after the temperature is higher than ~215 °C, suggesting that the coal–oxygen reactions are nearly independent of the oxygen concentration at relatively low temperatures. Similarly, it is found that ~209 °C and ~204 °C are the temperature points marking the divergence for 2 °C min<sup>-1</sup> and 1 °C min<sup>-1</sup>, respectively. The observation indicates that both the coal rank (composition) and the heating rate influence the inception of UCFs. Despite the small differences among the three heating rates, it can be inferred that the risk of coal spontaneous combustion is not reduced even in the oxygen-depleted environment.

To better delineate different reaction stages, a combined TGA–DTG result at the heating rate of 5 °C min<sup>-1</sup> under 21% oxygen concentration is shown in Fig. 3. Firstly, the point  $T_0$  is defined as the last peak before the DTG profile becomes stable [28]. From the initial temperature to  $T_0$ , drying is the dominant process, with some physical adsorption of oxygen as the secondary one.  $T_s$  on the figure denotes the point from which the various cases start to diverge, as illustrated in Fig. 2. Chemical adsorption of oxygen is the dominant process at the stage from  $T_0$  to  $T_s$ , and mass loss of the coal sample is insignificant at that stage [34]. Secondly,  $T_b$  is the burned-out temperature, corresponding to the first point where DTG=0. Thirdly,  $T_i$  is defined as the ignition temperature which can be

obtained from the intersection point of the tangents on the TGA profile [35]. The stage between  $T_s$  and  $T_b$  is marked as ‘Reactions’ and involves both devolatilization and oxidation.  $T_p$  is the point corresponding to the maximum of DTG, physically a turning point of the mass changing rate.

Based on the definitions of the characteristic temperatures discussed above, their values are obtained from the respective TGA and DTG results, as listed in Table 5. It is found that no significant difference in terms of  $T_i$  is observed, which clearly demonstrates its weak dependence on the oxygen concentration [36]. Another observation is that  $T_p$  decreases as the oxygen concentration increases, because the expression of the Arrhenius law tells that both the reaction temperature and the oxygen concentration determine the reaction rate. For a higher oxygen concentration, it requires a lower temperature to achieve the maximum mass loss value.

As to  $T_b$ , its overall magnitude increases with the increasing heating rate from  $1\text{ }^\circ\text{C min}^{-1}$  to  $5\text{ }^\circ\text{C min}^{-1}$ . To understand that observation, it should be noted that the total mass loss is a cumulative property, and a lower heating rate means a longer time to reach a certain temperature. As such, for the case with a higher heating rate it takes a shorter time (for integration) and a higher temperature (for reaction rate) to reach the boundary ( $T_b$ ) of the burned-out stage.

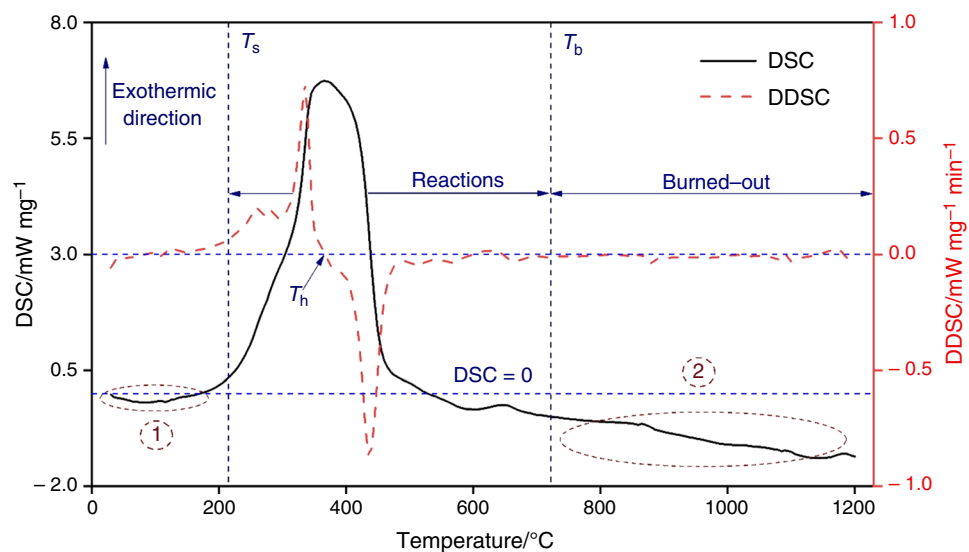
## Thermal behaviors

The DSC result represents the net heat generation, and differentiating it with respect to time, we obtain the DDSC result which indicates the ‘thermal acceleration.’ Figure 4 shows the combined DSC–DDSC results at  $5\text{ }^\circ\text{C min}^{-1}$  heating rate under 21% oxygen concentration. Two endothermic

**Table 5** Values of characteristic temperatures under different testing conditions

Heating rate	Oxygen concentration (%)	Characteristic temperature/ $^\circ\text{C}$				
		$T_0$	$T_s$	$T_i$	$T_p$	$T_b$
$1\text{ }^\circ\text{C min}^{-1}$	3	89	$\sim 204$	311	370	557
	9	91		311	357	548
	15	91		308	348	544
	21	91		307	343	542
$2\text{ }^\circ\text{C min}^{-1}$	3	99	$\sim 209$	315	423	713
	9	100		312	366	680
	15	101		312	349	671
	21	101		308	345	668
$5\text{ }^\circ\text{C min}^{-1}$	3	115	$\sim 215$	321	426	929
	9	113		316	385	729
	15	115		309	360	727
	21	115		307	340	722

**Fig. 4** DSC–DDSC result at  $5\text{ }^\circ\text{C min}^{-1}$  heating rate under 21% oxygen concentration



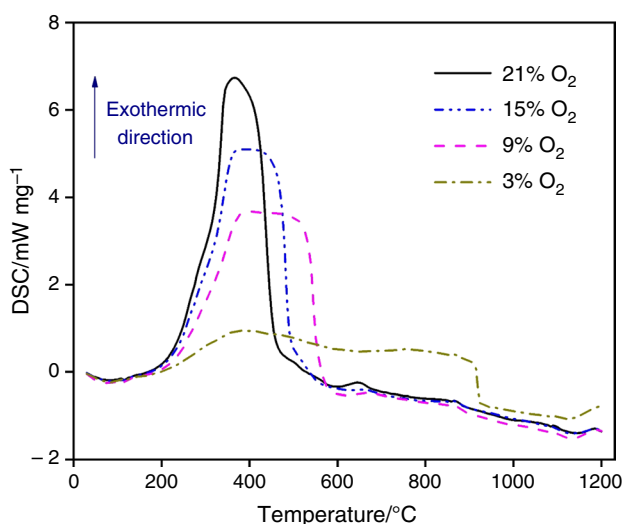


**Fig. 5** DSC results under different oxygen concentrations at  $5\text{ }^{\circ}\text{C min}^{-1}$  heating rate

regions (circled with numbers) are observed in the figure, one in the low-temperature zone and the other in the high-temperature zone. The one in the low-temperature zone mainly involves drying which consumes a lot of energy, while the one in the high-temperature zone is the result of mineral decomposition in the ash [32]. Here, another temperature, namely  $T_h$ , is defined as the point where DDSC = 0. Physically, it is the temperature at which heat generation reaches its maximum. Figure 5 reveals the effect of oxygen concentration on the DSC results. As can be seen, with the increasing oxygen concentration, the DSC profile becomes more protrusive and its peak value rises. For the extreme case of 3% oxygen concentration, the DSC result exhibits

a rather extended pattern with a relatively flat top. At the burned-out stage, the difference among the four cases diminishes again, suggesting its independence of the oxygen concentration. With the information given in Figs. 4 and 5, it is clearly indicated that the reaction rate (intensity) is greatly reduced with the decreasing oxygen concentration, while the duration of the ‘Reactions’ stage is significantly extended. That observation helps to understand why some coal seams could have been burning for a very long period of time: It is the limited oxygen supply that controls the reaction rate!

## Apparent activation energy

### Calculating method

Due to the complexity of coal–oxygen reactions, a global reaction approach which lumps detailed physicochemical processes is applied. In addition, drying and burned-out stages (mineral decomposition in ash) are not included in the calculation of the apparent activation energy. Only two stages (‘Oxygen adsorption’ and ‘Reactions’) are considered, as delineated in Fig. 3. According to the theory of chemical kinetics, the relationship between the apparent activation energy ( $E_a$ ) and the conversion rate ( $\alpha$ ) is very important. The conversion rate can be obtained from the sample mass expressed in Eq. (1):

$$\alpha = \frac{m_0 - m}{m_0 - m_\infty} \quad (1)$$

The Kissinger–Akahira–Sunose (KAS) method [37], which is used to calculate the apparent activation energy, is given by Eq. (2):

**Fig. 6** Calculated apparent activation energy as a function of temperature at  $5\text{ }^{\circ}\text{C min}^{-1}$  heating rate

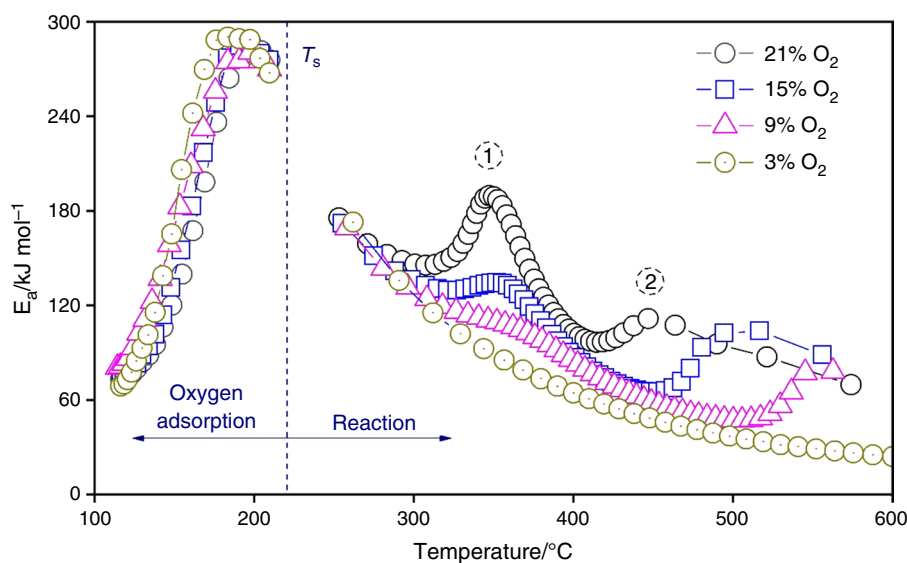
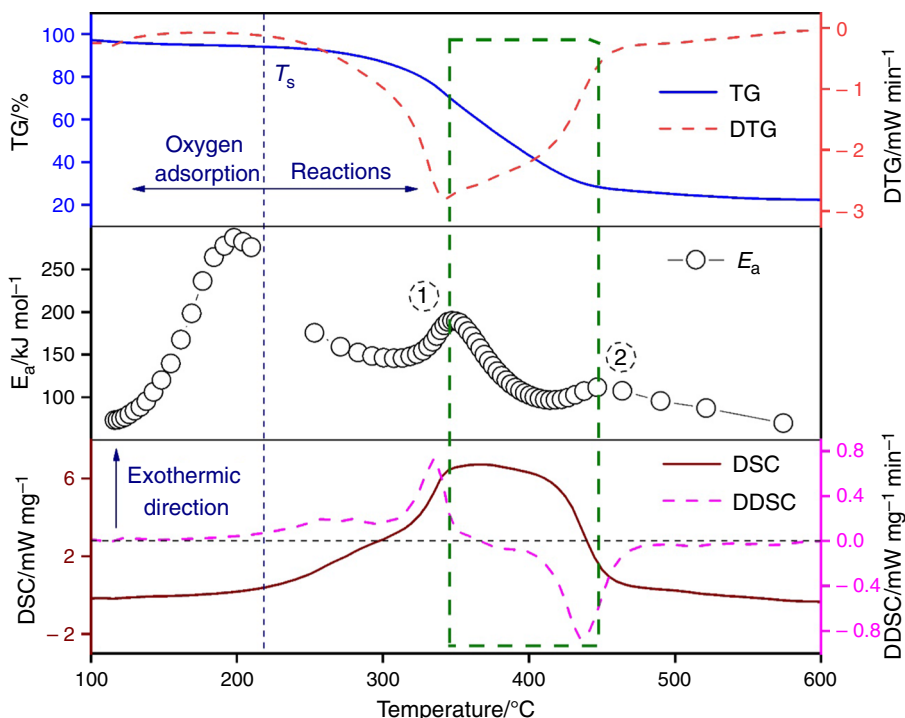
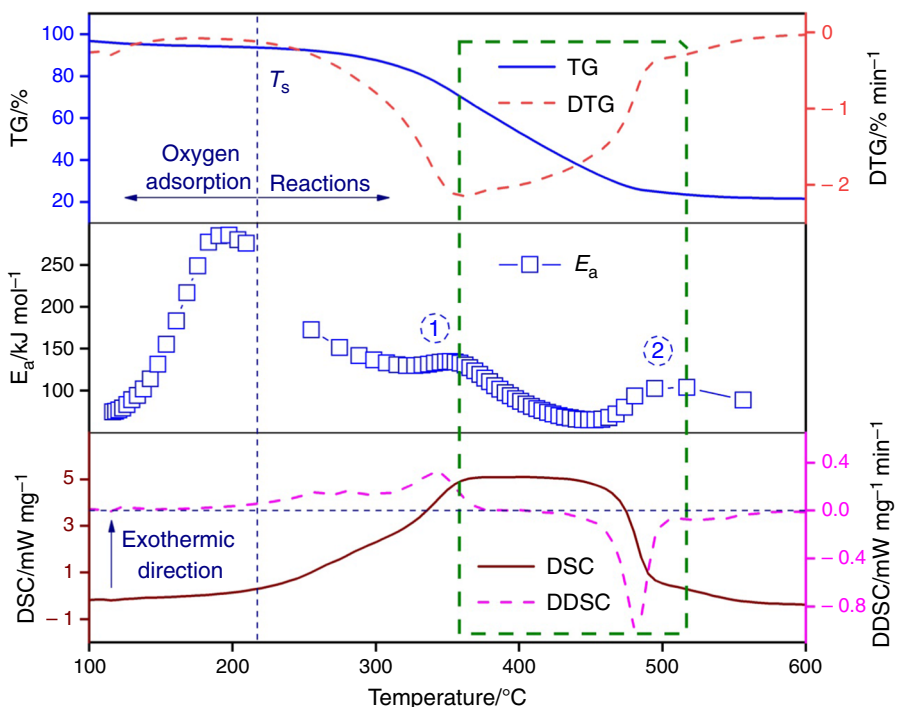


**Fig. 7** Composite diagram of TGA–DSC results with calculated apparent activation energy at 5 °C min<sup>-1</sup> heating rate



**(a)** 21% oxygen concentration



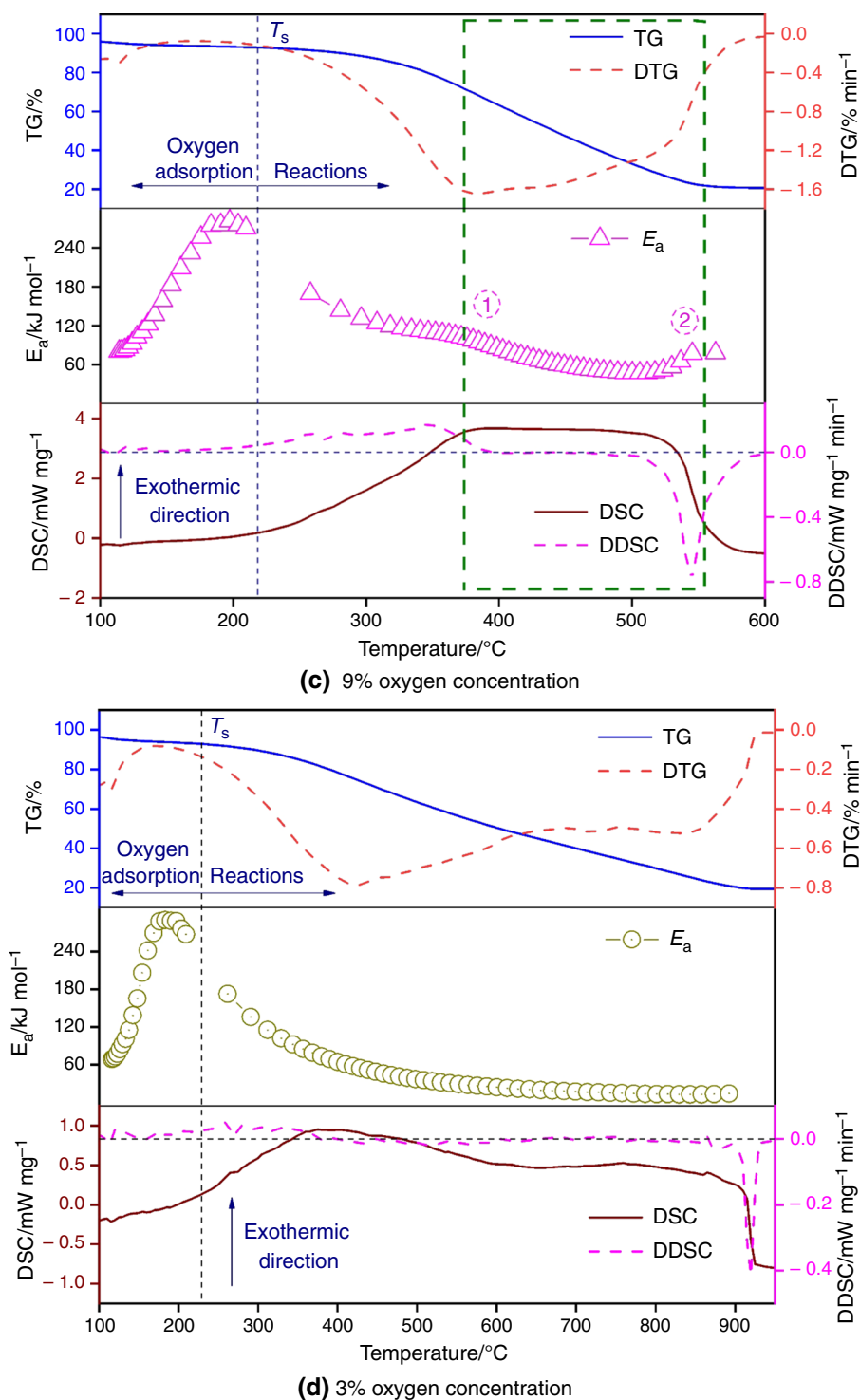
**(b)** 15% oxygen concentration

$$\ln\left(\frac{\beta}{T^2}\right) = \ln\left[\frac{A \cdot R_u}{E_a \cdot G(\alpha)}\right] - \frac{E_a}{R_u T} \quad (2)$$

where  $m_0$ ,  $m$  and  $m_\infty$  are the initial, instantaneous and final mass (in the unit of mg) of the coal sample, respectively;  $E_a$  is the apparent activation energy in the unit of kJ mol<sup>-1</sup>;  $A$

represents the pre-exponential factor in the unit of min<sup>-1</sup>;  $\beta$  is the heating rate in °C min<sup>-1</sup>;  $R_u$  is the universal gas constant,  $8.3145 \times 10^{-3}$  kJ mol<sup>-1</sup> K<sup>-1</sup>. With Eqs. (1) and (2),  $E_a$  can be obtained from the linear fitting of  $\ln(\beta/T^2)$  with  $1/T$ .

Fig. 7 (continued)



### Effect of oxygen concentration

With the procedure described above, the apparent activation energy is calculated and its variation with temperature is shown in Fig. 6. Generally, it can be seen that the major 'resistance' to the coal–oxygen reactions comes from the early stage of UCFs. Therefore, we can infer that measures

could be taken to prevent the self-ignition of coal, provided the low-temperature reactions could be effectively detected. Similar to the DTG results presented in Fig. 2, no significant difference in the apparent activation energy is found among the four cases at the 'Oxygen adsorption' stage. In contrast, at the 'Reactions' stage, the four oxygen concentrations exhibit sharply different patterns in terms of the



apparent activation energy. For 21% oxygen concentration, two humps are observed, as marked in Fig. 6. With the decrease in oxygen concentration, the magnitudes of those two humps gradually decline and both of them shift toward a higher-temperature region. For the extreme case of 3% oxygen concentration, the two humps almost disappear.

The first hump is believed to be the depletion of volatiles, and from that point onward, the char oxidation dominates the reactions. A higher oxygen concentration gives a higher reaction rate (intensity), and therefore the transition from volatiles burning to char oxidation occurs earlier (at a lower temperature). For 3% oxygen concentration, due to the rarely available oxygen, the reactions of both volatiles burning and char oxidation are of limited or very weak intensity, and oxygen transport is the limiting factor that controls the reaction rate. The second hump is speculated to be the nearly depletion of char. Thereafter, the remaining char inside the coal particles is burned out with the inward diffusion of oxygen. It should be mentioned that the above argument and the observation made from Fig. 6 could potentially lead to the ‘conception’ that a lower oxygen concentration is favorable in promoting coal–oxygen reactions, which is actually untrue. Looking at the expression of the Arrhenius law, the reaction rate is a function of  $E_a$  and the concentrations of reactants, in this case, the oxygen concentration. Even though the values of  $E_a$  are higher for higher oxygen concentrations, more abundantly available oxygen for reactions will outweigh the negative effect of a higher  $E_a$ , which ultimately leads to a higher reaction rate than the cases under lower oxygen concentrations, as shown by the DTG results in Fig. 2. With the changing oxygen concentration, Deng et al. [29] found a similar trend in terms of the relative magnitude of the apparent activation energy. They explained that the number of stable structures (in the coal) reacting with oxygen increases with the increase in oxygen concentration, which leads to the increase in the apparent activation energy.

### Macroscopic behaviors

In order to understand the macroscopic behaviors of coal–oxygen reactions, we combine the calculated apparent activation energy with the TGA–DSC results, and the composite diagrams are shown in Fig. 7. It is speculated in Sect. [Effect of oxygen concentration](#) that the physical meaning of the first hump is the depletion of volatiles, while the second is the depletion of char. The above speculation will be verified with the TGA–DSC results. For Fig. 7a, 7b and 7c, a green-squared region is highlighted in each diagram. It marks the region between the first and second humps on the profile of the apparent activation energy. It can be seen that in those regions the DTG goes up and the DSC is approaching zero at the end of the square. The ascending DTG indicates that the reaction rate is reduced over time, and the

inward diffusion of oxygen gradually becomes the limiting factor. At the end of the green-squared region, both DTG and DSC are approaching zero, manifesting the end of exothermic reactions. Overall, the width of the green-squared region increases with the decreasing oxygen concentration, which means that it takes a longer time to burn out the char under a lower oxygen concentration. For the extreme case of 3% oxygen concentration, the  $E_a$  profile exhibits an asymptotic pattern. From its DDSC curve, we can see very insignificant ‘thermal acceleration,’ from which it can be concluded that the reaction rate is very low due to the limited oxygen available.

### Conclusions

The coal–oxygen reactions occurring in UCFs are a very unique phenomenon due to the oxygen transport through the geological settings. To understand the inception and development of UCFs, a high-volatile brown coal sample is thermally analyzed with the combined TGA–DSC approach. Four oxygen concentrations and three heating rates are employed in the testing to reflect the actual conditions in UCFs. The noteworthy findings are summarized as follows:

- (1) Based on the TGA results, the reaction process is divided into four stages: drying, oxygen adsorption, reactions and burned-out. It is found that at the early stage of coal–oxygen reactions the dependence on the oxygen concentration is weak, suggesting that the danger of coal to spontaneous combustion is not reduced even in oxygen-depleted conditions.
- (2) Based on the KAS method, the apparent activation energy is calculated and two humps are observed at the ‘Reactions’ stage, which physically marks the transition from volatiles burning to char oxidation. The oxygen concentration significantly influences the reaction progress and intensity at that stage, with the magnitudes of those two humps gradually declining and both of them shifting toward a higher-temperature region.
- (3) Compared to the other three cases, the extreme case of 3% oxygen concentration shows very distinct macroscopic thermochemical behaviors, which is identified from a rather flat top of DSC peak as well as the asymptotic pattern of apparent activation energy (disappearance of humps), demonstrating the unique characteristics of coal–oxygen reactions which are mainly controlled by the oxygen diffusion throughout the entire process.

**Acknowledgements** The authors gratefully acknowledge the financial support provided by the National Natural Science Foundation of China

(Grant No. 51850410504) and Open Projects of State Key Laboratory of Coal Resources and Safe Mining of CUMT (Grant No. 14KF01).

## References

- Kuenzer C, Zhang J, Tetzlaff A, van Dijk P, Voigt S, Mehl H, *et al.* Uncontrolled coal fires and their environmental impacts: Investigating two arid mining regions in north-central China. *Appl Geogr.* 2007;27:42–62.
- Stracher GB, Taylor TP. Coal fires burning out of control around the world: thermodynamic recipe for environmental catastrophe. *Int J Coal Geol.* 2004;59:7–17.
- Melody SM, Johnston FH. Coal mine fires and human health: What do we know? *Int J Coal Geol.* 2015;152:1–14.
- Zhang Y, Li Y, Huang Y, Li S, Wang W. Characteristics of mass, heat and gaseous products during coal spontaneous combustion using TG/DSC–FTIR technology. *J Therm Anal Calorim.* 2017;131:2963–74.
- Tang Y, Wang H. Experimental investigation on microstructure evolution and spontaneous combustion properties of secondary oxidation of lignite. *Process Saf Environ.* 2019;124:143–50.
- Carras JN, Young BC. Self-heating of coal and related materials: models, application and test methods. *Prog Energy Combust.* 1994;20:1–15.
- Wang H, Dlugogorski BZ, Kennedy EM. Coal oxidation at low temperatures: oxygen consumption, oxidation products, reaction mechanism and kinetic modelling. *Prog Energy Combust.* 2003;29:487–513.
- Green U, Aizenshtat Z, Metzger L, Cohen H. Field and Laboratory Simulation Study of Hot Spots in Stockpiled Bituminous Coal. *Energ Fuel.* 2012;26:7230–5.
- Zhang Y, Wu J, Chang L, Wang J, Xue S. Kinetic and thermodynamic studies on the mechanism of low-temperature oxidation of coal: A case study of Shendong coal (China). *Int J Coal Geol.* 2013;120:41–9.
- Wang H, Dlugogorski BZ, Kennedy EM. Examination of CO<sub>2</sub>, CO, and H<sub>2</sub>O Formation during low-temperature oxidation of a Bituminous Coal. *Energ Fuel.* 2002;16:586–92.
- Dong X, Wen Z, Wang F, Meng Y. Law of gas production during coal heating oxidation. *Int J Min Sci Techno.* 2019;29:617–20.
- Yang Y, Li Z, Hou S, Gu F, Gao S, Tang Y. The shortest period of coal spontaneous combustion on the basis of oxidative heat release intensity. *Int J Min Sci Techno.* 2014;24:99–103.
- Jayaraman K, Gökalp I. Thermal characterization, gasification and kinetic studies of different sized Indian coal and char particles. *Int J Eng Sci.* 2014;6:31–40.
- Song Z, Huang X, Luo M, Gong J, Pan X. Experimental study on the diffusion–kinetics interaction in heterogeneous reaction of coal. *J Therm Anal Calorim.* 2017;129:1625–37.
- Wang D, Xin H, Qi X, Dou G, Qi G, Ma L. Reaction pathway of coal oxidation at low temperatures: a model of cyclic chain reactions and kinetic characteristics. *Combust Flame.* 2016;163:447–60.
- Arisoy A, Beamish B. Reaction kinetics of coal oxidation at low temperatures. *Fuel.* 2015;159:412–7.
- Kim CJ, Sohn CH. A novel method to suppress spontaneous ignition of coal stockpiles in a coal storage yard. *Fuel Process Technol.* 2012;100:73–83.
- Rosema A, Guan H, Veld H. Simulation of spontaneous combustion, to study the causes of coal fires in the Rujigou Basin. *Fuel.* 2001;80:7–16.
- Song Z, Wu D, Jiang J, Pan X. Thermo-solutal buoyancy driven air flow through thermally decomposed thin porous media in a U-shaped channel: Towards understanding persistent underground coal fires. *Appl Therm Eng.* 2019;159:113948.
- Song Z, Huang X, Jiang J, Pan X. A laboratory approach to CO<sub>2</sub> and CO emission factors from underground coal fires. *Int J Coal Geol.* 2020;219:103382.
- Yang J, Liu N, Chen H, Gao W, Tu R. Effects of atmospheric oxygen on horizontal peat smoldering fires: Experimental and numerical study. *Proc Combust Inst.* 2018;37:4063–71.
- Qi G, Wang D, Zheng K, Tang Y, Lu X. Smoldering combustion of coal under forced air flow: experimental investigation. *J Fire Sci.* 2016;34:267–88.
- Song Z, Kuenzer C. Coal fires in China over the last decade: A comprehensive review. *Int J Coal Geol.* 2014;133:72–99.
- Kök M. Recent developments in the application of thermal analysis techniques in fossil fuels. *J Therm Anal Calorim.* 2008;91:763–73.
- Russell N, Beeley T, Man CK, Gibbins J, Williamson J. Development of TG measurements of intrinsic char combustion reactivity for industrial and research purposes. *Fuel Process Technol.* 1998;57:113–30.
- Li J, Fu P, Mao Y, Saini V, Sokol E. A Parametric Study on the Inception and Evolution of Underground Coal Fires Based on a Lab-Scale Experimental Setup. *Fire Technol.* 2019;56:1039–57.
- Qi X, Li Q, Zhang H, Xin H. Thermodynamic characteristics of coal reaction under low oxygen concentration conditions. *J Energy Inst.* 2017;90:544–55.
- Li Z, Zhang Y, Jing X, Zhang Y, Chang L. Insight into the intrinsic reaction of brown coal oxidation at low temperature: Differential scanning calorimetry study. *Fuel Process Technol.* 2016;147:64–70.
- Deng J, Li Q, Xiao Y, Wen H. The effect of oxygen concentration on the non-isothermal combustion of coal. *Thermochim Acta.* 2017;653:106–15.
- Qi G, Wang D, Zheng K, Xu J, Qi X, Zhong X. Kinetics characteristics of coal low-temperature oxidation in oxygen-depleted air. *J Loss Prevent Proc.* 2015;35:224–31.
- Li Q, Xiao Y, Wang C, Deng J, Shu C. Thermokinetic characteristics of coal spontaneous combustion based on thermogravimetric analysis. *Fuel.* 2019;250:235–44.
- Naktiyok J. Determination of the self-heating temperature of coal by means of TGA analysis. *Energ Fuel.* 2018;32:2299–305.
- Li X, Li C, Zhang H, Li W. Analysis on the status and problems of lignite application in China. *Appl Chem Ind.* 2020;49:1226–30 (**[in Chinese]**).
- Xin H, Wang H, Kang W, Di C, Qi X, Zhong X, *et al.* The reburning thermal characteristics of residual structure of lignite pyrolysis. *Fuel.* 2020;259:116226.
- Wang C, Zhang X, Liu Y, Che D. Pyrolysis and combustion characteristics of coals in oxy-fuel combustion. *Appl Energy.* 2012;97:264–73.
- Liu Y, Cao X, Duan X, Wang Y, Che D. Thermal analysis on combustion characteristics of predried dyeing sludge. *Appl Therm Eng.* 2018;140:158–65.
- Vyazovkin S, Burnham AK, Criado JM, Pérez-Maqueda LA, Popescu C, Sbirrazzuoli N. ICTAC Kinetics Committee recommendations for performing kinetic computations on thermal analysis data. *Thermochim Acta.* 2011;520:1–1.

**Publisher's Note** Springer Nature remains neutral with regard to jurisdictional claims in published maps and institutional affiliations.